A New Monoplotting Tool to Extract Georeferenced Vector Data and Orthorectified Raster Data from Oblique Non-Metric Photographs

by
C. Bozzini, M. Conedera, P. Krebs

Reprinted from

International Journal of
Heritage in the Digital Era

volume 1 number 3 2012

A New Monoplotting Tool to Extract Georeferenced Vector Data and Orthorectified Raster Data from Oblique Non-Metric Photographs

C. Bozzini[a, *], M. Conedera[a], P. Krebs[a]

[a]Swiss Federal Research Institute WSL, Insubric Ecosystem Research Group, CH-6500 Bellinzona, Switzerland

(claudio.bozzini, marco.conedera, patrik.krebs)@wsl.ch

* Corresponding author.

A New Monoplotting Tool to Extract Georeferenced Vector Data and Orthorectified Raster Data from Oblique Non-Metric Photographs

C. Bozzini, M. Conedera, P. Krebs

Abstract:

Since its invention in the first half of the nineteenth century, photography has assumed a leading role as a means for documenting the real world. With the improvement of technology, photography developed into photogrammetry, enabling the mapping and georeferencing of landscape elements beginning with stereo photographs. With the introduction of aerial photography, terrestrial oblique photography became obsolete for cartographic purposes and was nearly forgotten by most specialists in photogrammetry. In recent times, the improvement of computing power and the production of high resolution Digital Elevation Models has made the spatial georeferincing of single oblique pictures (monoplotting) more approachable. In this paper, we focus on a new monoplotting tool developed by our research group and we illustrate the basic concept, the solutions implemented and options as well as the results of a case study on land-use and vegetation evolution over a 100-year period. The tool has been conceived to georeference ordinary individual photographs in order to orthorectify the visible landscape or to produce and export map layers (e.g. georeferenced vector data) by drawing them directly on these pictures. The basic requirements of the system are the digital version of the historical picture, the DEM of the depicted landscape, the real-world coordinates of a suitable number of control points unambiguously

recognizable on the picture, and – suitable but not mandatory - the real-world coordinates of the precise shooting point and of the centre of the picture.

Key words: monoplotting, photogrammetry, old photographs, camera model, digital elevation model

1. Introduction

1.1 Why monophotogrammetry?

Developed in the first half of the nineteenth century, photograhy soon became a very effective method of documenting landscape features and dynamics. As a result, many large collections of old photographs in public or private archives exist, representing an enormous resource for the study of landscape evolution and land use change (Kull, 2005; Hendric and Copenheaver, 2009; Nyssen et al., 2009). In addition, the quality of these historical pictures is often impressive owing to the very high resolution that was possible using photographic glass plates and other classic types of support and film. Unfortunately, on account of the difficulties in obtaining quantitative geographical data from single oblique pictures, this resource long remained unexploited by most researchers in historical geography. In fact, reconstructions of landscape history are often based on the analysis of old maps or aerial photographs.

Nevertheless, it is unquestioned that terrestrial historical photographs present numerous advantages. Most old specimens allow detailed views of landscapes dating back to the late 1800s and early 1900s, that is, several decades before the advent of aerial photography. They are easier to interpret, reflecting our everyday perception and experience of the environment, and they may provide high resolution and more details, as in the case of pictures taken from the opposite slope in mountain regions (Krebs and Conedera, 2004) and where possible rephotography is very low in terms of cost.

In recent times, the general increase in computing power (Ceruzzi, 2003), the improvements in digital elevation models (DEM) (Miller and Laflamme, 1958; Hodgson and Bresnahan, 2004), as well as the implementation of user-friendly and versatile releases of the Geographic Information Systems (GIS) have opened new perspectives for a broad use of single terrestrial oblique pictures for photogrammetric purposes (monoplotting). After the pioneer work of

Makarovič (1973, 1982), several attempts have been made to develop software and tools for monoplotting oblique pictures. These include the OP-XFORM project (Doytsher and Hall, 1995), the JUKE method (Aschenwald et al., 2001), Georeferencing oblique terrestrial photography (Corripio, 2004), the 3D Monoplotter (Mitishita et al., 2004), and the DiMoTeP (Fluehler et al., 2005). None of these products, however, really meet the needs of potential end-users in terms of operational flexibility and user-friendliness of the interface, which, in the final analysis, greatly inhibit their broad use.

Recent further improvements in techniques in digitalizing historical pictures and the availability of high performance digital cameras, make the development of a specific and user-friendly monoplotting tool more interesting and necessary. We therefore started developing a new monoplotting interface in 2010, with the aim of offering an intuitive platform for georeferencing recent and historical terrestrial oblique photographs to a broad number of non-expert potential users.

1.2 Aim of the paper

The aim of this paper is first to present the basic concepts and features of the monoplotting tool as well as the data and procedures needed to set up the system.

In the second part, we report on the results of a study case consisting in using past and present terrestrial pictures and a historic vegetation map to quantitatively and qualitatively reconstruct land-use and vegetation changes over the last 100 years in a remote valley of southern Switzerland.

2. The WSL Monoplotting Tool

2.1 Monoplotting principle

Photogrammetry is usually and implicitly intended to mean stereophotogrammetry, or specifically the technique for collecting or extracting 3D data or information from two overlapping aerial photographs (also called stereo pair). The extraction technique usually implies that all camera parameters (intrinsic and extrinsic) are well-known (Wolf and Dewitt, 2000; Mikhail et al., 2001). In contrast to this, mono-photogrammetry or monoplotting represents a photogrammetric system where single oblique and unrectified photographs or aerial (nadir) images are related to the digital elevation models (DEM) of the corresponding real world (Figure 1). In practical terms the camera, the picture and the DEM are related to each other so that a line from the camera center and passing through a selected point in the picture plane will intersect the land surface (DEM) in the corresponding real point (Figure 2). An important difference between the two systems is that, while stereo-phogrammetry enables the calculation of the position of any point within the camera's field of view, in mono-photogrammetry only points located on the land surface (DEM-surface) can be precisely located.

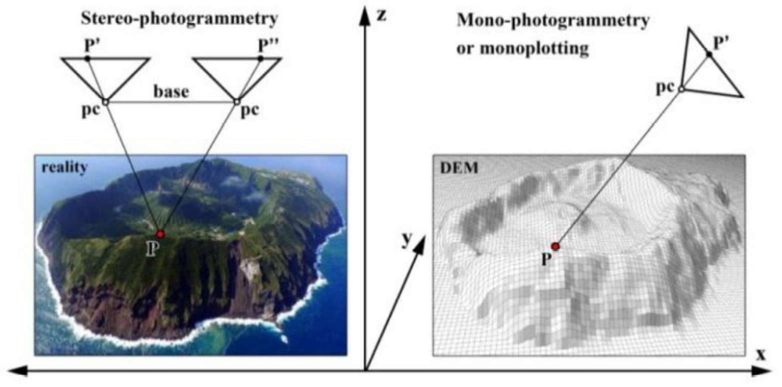

Figure 1: Principles of stereo- and mono-photogrammetry applied to the Japanese volcanic island of Aogashima (adapted from Waldhäusl and Hochstöger (1990, p. 137).

Legend: pc = projection centre; P = object point; P' = representation of P in the first photo; P'' = representation of P in the second photo; base = distance between the projection centers of the stereo pair.

2.2 Basic requirements of the tool

We defined the main requirements for a monoplotting tool as the following:

- A user-friendly and self-explanatory interface enabling a simultaneous visualization of photographs and maps, orthophotos or other cartographic support of the corresponding landscape.
- Computer assisted semi-automatic calibration of the camera, including reconstruction of the original snapshot point.
- Tools for georeferencing and measuring different features (polygons, lines, heights etc.) directly on the oblique photographs.
- Export–import routines for exchanging data (e.g. shapefiles) with conventional geographic information systems.
- Error estimation for each calculated point on the oblique photograph.
- Orthorectifying of every photographic pixel, viz. the transposition of the oblique picture into a orthophoto and vice versa.

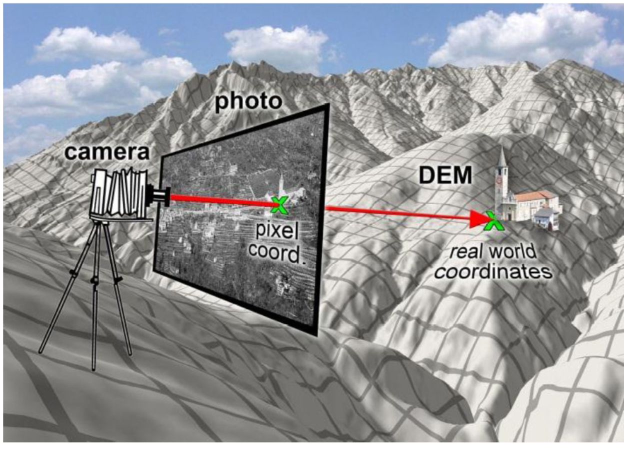

Figure 2: Implementation of a monoplotting system.

2.3 Input data

The monoplotting system requires the following input data:

1. **A Digital image** derived from modern digital cameras or from scanned old pictures (e.g. historic photos on glass plates, negative films, reversal films, postcards, etc.). The monoplotting system accepts photos resulting from any type of camera and lens, even small-format and non-metric cameras. Camera and lens characteristics may however influence the final accuracy of the system.
2. **A Digital Elevation Model (DEM)**, best when represented by a regularly spaced grid (e.g. raster in geotiff format). The following two options are possible: a bare ground surface without any objects (Digital Terrain Model: DTM) or the earth's surface including objects such as plants and buildings (Digital Surface Model: DSM).
3. **Control points (CPs)** clearly and precisely identifiable on both the photograph (pixel coordinates) and the real world (world coordinates latitude, longitude, and altitude). CPs typically consist of unambiguous features that may be pinpointed at pixel level on the photo, such as road and footpath intersections, rocky outcrops, building or wall corners, and other permanent, visible, natural or anthropogenic elements. CPs should be at least four or more in number, fairly homogeneously distributed across the entire photograph, and possibly (but not necessarily) placed on the ground (DTM). The real coordinates of the CPs can be directly measured in the field using surveying instruments (e.g. GNSS, total stations) or indirectly derived by orthorectifying geographical data (e.g. maps, DTM, DSM, orthophotos, cadastral surveys, etc.).

2.4 System implementation

The first step in initializing the monoplotting system is the camera calibration, or more precisely the calculation, estimation and simulation of the 11 extrinsic and intrinsic camera parameters as postulated by Kraus (1993) (Table 1). In our tool, camera calibration is addressed through an iterative approach, generating a sequence of improving approximations of the camera parameters that minimize the error of the camera model applied to the input data. The iterative approach consists of the application of collinearity equations commonly used in photogrammetry (Ghosh, 2005), including the estimation of unknown camera parameters by the mean of the least square method after a linearization of the collinearity equations (Strausz, 2001).

Table 1: Camera parameters.

Extrinsic (exterior) parameters	
defining the location and the orientation of the camera	
xc yc zc	Real word coordinates of the projection centre (perspective centre or pinhole), i.e. the point inside the lens where all light rays intersect
γ (roll/x-axis) β (tilt/y-axis) α (pan/z-axis)	Euler rotation angle describing the camera orientation around the correspondent axis
Intrinsic (internal) parameters	
defining the internal properties of the photographic image	
xp yp	Pixel coordinates of the image centre (principal point) that is the point where the optical axis (the line perpendicular to the image plane passing through the projection centre) intersects the imaging surface
f (or c)	The principal distance, which is the perpendicular distance from the image to the projection centre. This distance is equal to the focal length with the lens focused at infinity
k1, …, k3 (radial) p1, p2 (tangential)	Lens distortion parameters due to imperfections in the lenses, viz. differences between the optical system and the predictions of paraxial optics (orthoscopic vision)

When CPs are precisely located (required precision highly depends on the single case) and well arranged on both the photo and the real space, usually the algorithm converges automatically towards the best solution. Conversely, when the CPs are suboptimal or when the photos do not exactly correspond to a plane projection of reality (owing to film unflatness, particular lens distortions or other irregularities during photo reproduction or photo scanning), the algorithm may converge towards a local minimum that isn't the best solution, or in the worst cases, the algorithm can even continue to loop without going toward a solution (Samtaney, 1999, pp. 10-11). In these cases, it may be necessary to verify the integrity of the input data, or it can be useful to try to reduce the number of unknown parameters by defining some suitable initial values, for instance, by providing a first approximation of the camera position (3D coordinates) to the software. Other times, it may be necessary to manually correct some parameters, for example, by completely reversing the camera orientation (i.e. with a rotation of 180 degrees) to solve the problem of two symmetrical solutions that often arises even when CPs are precise, numerous and well distributed.

When the camera calibration is successfully achieved, the tool generates a model of all the extrinsic and intrinsic camera parameters, thereby simulating the true setup of the camera and the real conditions under which the photo was taken.

2.5 Achieved precision

The reliability of the system and the precision of the results are clearly affected by the quality of the photograph (e.g. low resolution, lens distortion, film unflatness), the number, precision and the distribution of control points, the accuracy of the DEM (e.g. resolution of 2 m or higher, no mass movements since the time of the picture), the accuracy of the camera calibration and the angle of incidence of the optical ray on the DEM surface (in general, the higher the angle of incidence, the higher the obtained precision). According to these frame conditions, the monoplotting system may achieve precision levels ranging from less than a meter to decameters.

3. The Case Study of the Onsernone Valley

3.1 The Onsernone Valley

The research area is the 25 km long Onsernone valley, trending east-west, near Lago Maggiore in the southern Alps of Switzerland (Figure 3). The valley is v-shaped, deeply incised in siliceous (gneiss) bedrock, and characterized by steep lateral slopes interrupted by four terrace systems (Canale, 1958). The elevation gradient is huge, ranging from 250 m asl (Melezza River) to 2551 m asl (Pizzo di Madei). The mean annual temperature is 11°C, whereas annual precipitation is about 2,000 mm on average, with dry winters and a nearly bimodal regime with peaks in spring and fall. The valley's south-facing slopes are generally covered by a mixed hardwood forest, dominated by the European chestnut (*Castanea sativa*) whereas European beech (*Fagus sylvatica*) prevails on north-facing slopes.

Prior to the 20th Century, due to the geomorphologically harsh conditions, large settlements and main agricultural activities were concentrated on terraces on the south-facing slopes. The remaining territory was mostly used as pasture land and for timber and charcoal

Figure 3: The research area in southern Switzerland.

production. The economic profitability of such agro-pastoral land-use declined progressively during the first half of the 20th century and completely collapsed after the Second World War giving rise to a marked recolonization of the territory by tree forest species (Muster et al., 2007).

3.2 Photographic and cartographic materials

3.2.1 Vegetation map of 1905-1918

At the beginning of the 20th century, the vegetation in the Onsernone Valley was carefully studied and described by the botanist Johann Bär (1877-1957) through countless surveys in the field (especially between 1905 and 1909). The final product resulted in a publication that included a detailed 1:50,000 scale colour map (Bär 1918) with considerable detail on the vegetation cover through a complex and partially superimposed legend of many different symbols and colours. A high resolution (600dpi) scan (Epson Perfection V700 Photo) of the map allowed us to transfer all of this rich information into a TIF format digital copy that was subsequently georeferenced using local stretch transformations in *AirPhoto* (v. 3.56) and georeferencing tools in *ArcMap* (v. 10).

3.2.2 The Zinggeler's pictures of 1933

The photographer Rudolf Zinggeler (1864-1954) visited the Onsernone Valley and produced (especially in 1933) several glass plates with close-ups of people and buildings but also with large scenic views showing vegetation cover on the mountain slopes. We selected three landscape-relevant photographs from the Zinggeler collection presently preserved at the Federal Archive of historical monuments (FAHM) in the National Library in Bern, which provided us with high resolution digital copies of the selected negative images. The images were then optimized with *Photoshop CS5* using different filters and zonal adjustments (brightness, contrast, levels) in order to maximize the information related to landscape and vegetation elements.

3.2.3 The rephotographs of 2012

On April 18th, 2012 we rephotographed Zinggeler's photos using a digital camera (Canon 550D) mounted on a tripod (Manfrotto 055XDB) equipped with a 3-way pan-tilt head (Manfrotto 804RC2). Whenever possible, we shot the 2012 photos from the exactly same position. If the original shooting point presented some problems (new trees or buildings covering the field of vision) we took the new photos from an alternative nearby position offering a good panoramic view. In order to maximize resolution, for every shooting point we created a mosaic of photographs using several overlapping detail photos taken from the same location and adapted to the same wide-angle photo perspective.

3.3 Image selection, treatment and analysis

3.3.1 Image selection

After comparing the photographic material collected, we chose three pairs of images, each comprising a Zinggeler photo and the corresponding mosaic of current photos. Each of these photo pairs shows well the appearance and evolution of the vegetation in a particular area of the Onsernone Valley.

Zinggeler photo no.	nearest village	area (ha)	elevation range (m asl)	mean aspect	mean slope
5012	Crana	9.20	1030-1600	ENE	44.8°
5182	Gresso	39.02	960-1750	NNE	36.8°
5206	Vergeletto	11.49	930-1310	SSW	44.0°

Table 2: The three study areas. Orthogonal area, elevation range, aspect and mean slope have been calculated for the surface terrain inside the shared frame (see below).

3.3.2 Defining a shared landscape frame

For every selected photo (three historic photos and three rephotographs), we defined the landscape frame that offered the best conditions in terms of photo interpretation. Then, for every historic and new photo pair, we used our monoplotting tool to project the frame defined on the new photo onto the historic photo. This allowed the comparison of the *"new frame"* with the *"old frame"* and the definition of the *"shared frame"*, that is, the portion of the territory clearly visible on both the historic and the new photo. The obtained shared frames were also projected orthogonally and placed upon the georeferenced vegetation map. Then, using *ArcMap*, we calculated the viewshed for every old and new photo, that is a binary raster identifying which pixels or cells of the territory surface can be seen from the observation point according to the digital elevation model. The next step consisted of calculating the "shared viewshed", which is a binary raster that identifies the visible cells in both the old and new viewshed and located inside the planar projection of the shared frame.

3.3.3 Defining the vegetation cover

Mapping of the vegetation cover was done inside the three shared frames by using both their photographic and planimetric projections. The interpretation of the vegetation on both old and new pictures did not reach the detail level provided by Bär's vegetation map. Nevertheless, we tried to make the vegetation categories from the map compatible with the resulting data from the photo interpretation. The limits of the vegetation types recognized were then drawn directly on the terrestrial pictures (1933 and 2012) and on the vegetation map, and transformed into polygons. This was done using *ArcMap* starting from the shared frame and using the editing tools with some particular procedures (e.g. *"Cut Polygon"* and *"Snapping"* functions) in order to create clean shapefile-polygons with perfectly contiguous features that share coincident boundaries. In other cases, we preferred to use *Photoshop* to trace out these boundaries, saving them as PNG files with indexed colours. These files were then transformed into shapefiles using the *"Raster to Polygon"* function in *ArcMap* with the option *"Simplify polygons"* enabled. The real word coordinates of these polygons were then calculated through the WSL monoplotting tool.

3.3.4 Quantifying the evolution of the vegetation cover

All the georeferenced polygons of the recognized vegetation categories were then imported into *ArcMap* and compared to the corresponding shared viewshed. For every image (map, old and new photos) and for every recognized vegetation category, we calculated a binary raster bitmap which represented the intersection of the georeferenced polygon with the shared viewshed. This was done by rasterizing the polygons (vector to raster conversion) and by removing all the cells not included in the shared viewshed. By applying the *"DEM Surface Tools"* (an extension developed by Jeff Jenness) and the *"Sample"* function of *ArcMap* (Spatial Analyst Tools) to the produced bitmaps, we calculated the orthogonal and surface area (i.e. the area of the curved surface of the DEM) for every vegetation category in every image produced.

4. Results and Discussion

Figures 4, 5 and 6 reproduce different perspectives for every study area of the mapped vegetation categories in the three time periods considered, in order to enable an immediate comparison of the othogonal and the photographic views.

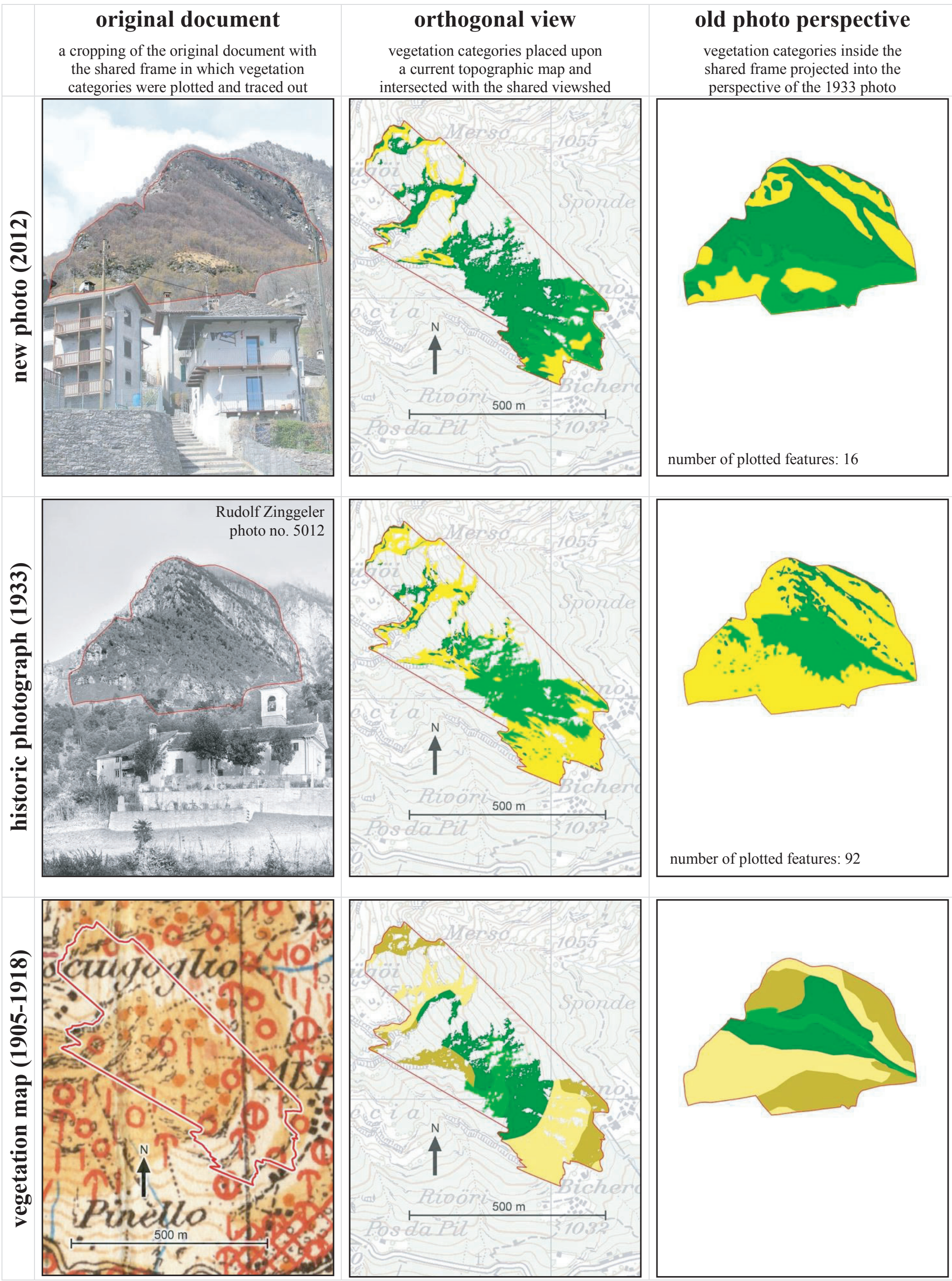

Figure 4: Evolution of the vegetation cover on a mountainside above the village of Crana.
Red contours represent the shared frame, coloured pixels represent the shared viewshed; for the colour legend, see Fig. 7.
For the photo images, the number of single features (polygons) detected is given.

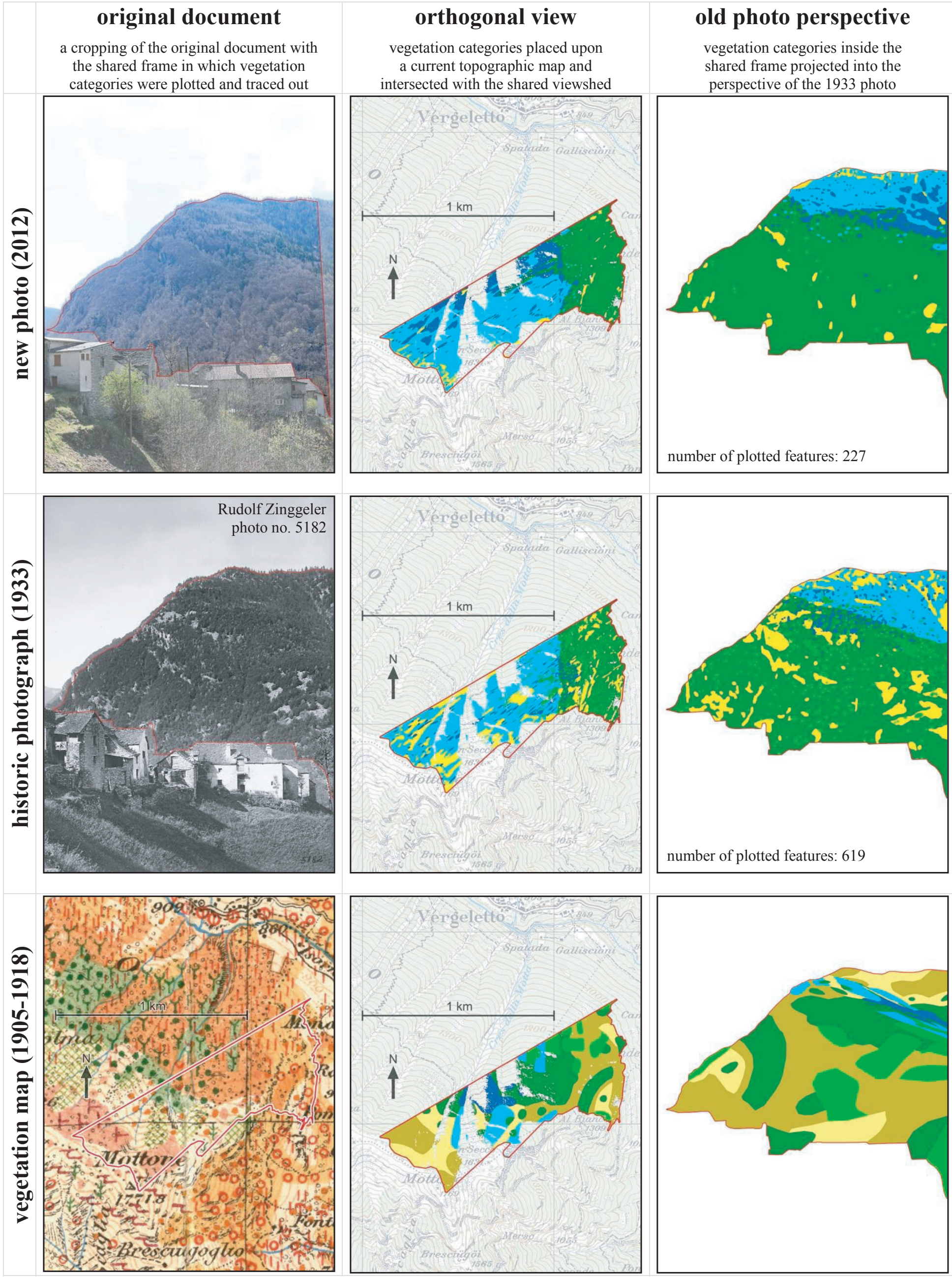

Figure 5: Evolution of the vegetation cover on a mountainside opposite the village of Gresso. Red contours represent the shared frame, coloured pixel represents the shared viewshed; for colour legend, see Fig. 7. For the photo images, the number of single features (polygons) detected is given.

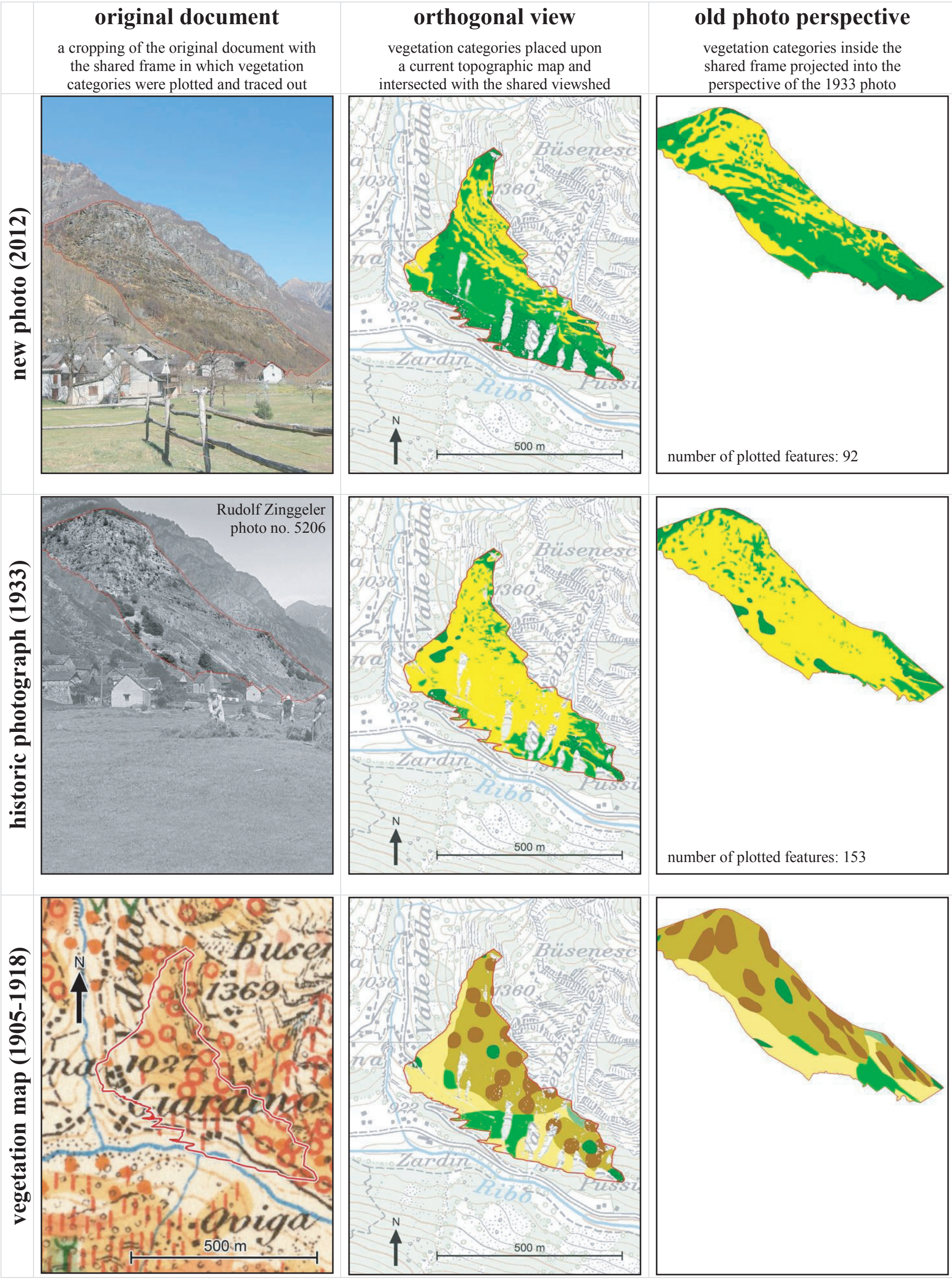

Figure 6: Evolution of the vegetation cover on a mountainside above the village of Vergeletto. Red contours represent the shared frame, coloured pixels represent the shared viewshed; for the colour legend, see Fig. 7. For the photo images, the number of single features (polygons) detected is given.

Figure 7 summarizes the different categories of vegetation cover we obtained from the different sources we used. On Bär's old map, 9 vegetation categories are defined. On the corresponding photos, we were able to retain only 5 vegetation categories. In particular, only a pasture type and two late successional stand types (a - broad-leaved species; b - evergreen coniferous species) have been recognized on the images. All the defined vegetation categories can easily be grouped into three overall categories simulating the effects of the abandonment of the pasture land: pasture, pioneer forest stands, and late successional stands.

Figure 7: Colour legend for the defined vegetation categories.

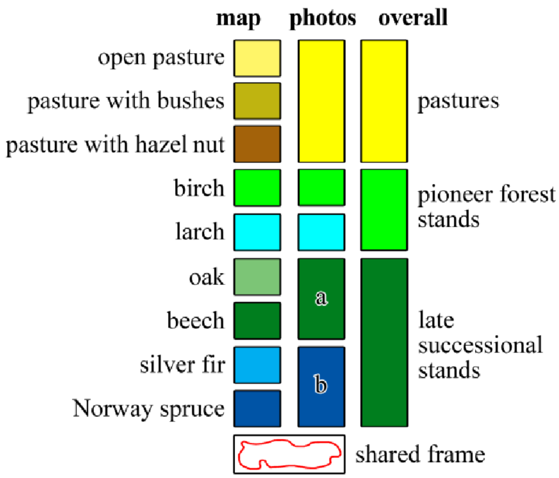

These vegetation categories, that were plotted directly onto the photos, were then converted successfully to the planimetric projection system thanks to our WSL monoplotting tool. After that, it was easy to calculate their orthogonal and surface area using *ArcMap* together with the *DEM Surface Tools* extension. Since the slope is rather steep in the three study areas (Table 2), the surface area is much greater than the flat area, but the relative values (percentages) for every vegetation category remain roughly unchanged (data not shown). We therefore preferred to present and discuss only the values of the orthogonal areas in percentages for each vegetation category.

The overall evolution of the vegetation cover for the whole study area is marked by the same general trend. Over a period of a century, pasture surfaces have diminished drastically from 58% to 10% (Figure 8). In 2012, more than half of the area (52%) is represented by late successional forest stands (especially beech but also evergreen conifers).

In general, the structure of the vegetation cover has become simpler and more monotonous with a noticeable decline in the total

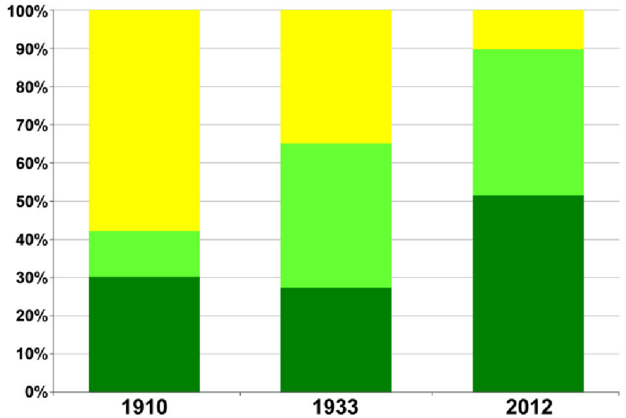

Figure 8: Overall evolution of the vegetation cover in the three study areas (100% = 59.71 ha = sum of total orthogonal area of the shared viewsheds in the three study area).

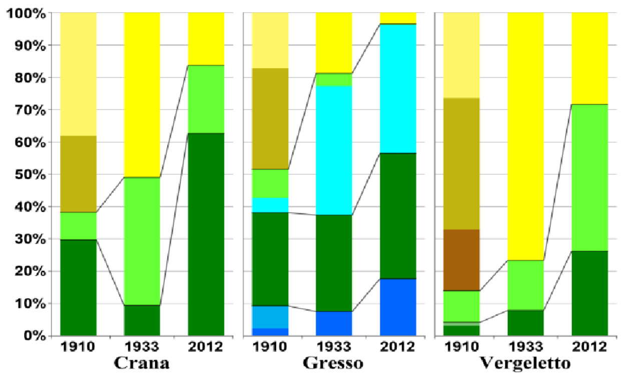

Figure 9: Percentage evolution of the detailed vegetation categories in the single study areas (100% = total orthogonal area of the shared viewsheds for each study area).

number of elements in the mosaic of vegetation units. In the three study areas, the total number of these units decreased from 864 to 335 between 1933 and 2012 (see the number of plotted features in Figures 4, 5, and 6).

Similarly, combining the analysis of the photographic images and maps (Figures 4, 5, and 6) with the detailed results of the vegetation cover evolution at the single area level (Figure 9), additional insights into the vegetation dynamics can be revealed.

Over the whole study area and the whole time period considered, the total area occupied by broadleaved pioneer stands has remained more or less unchanged, but migrated from the most remote and marginal zones towards the proximity of the villages (e.g. Figures 4 and 6).

The presence of coniferous forests is limited to the high elevation part of the north-facing area (Gresso). Larch in particular is confined to the former pasture lands at high altitude and still resists the penetration of late successional, evergreen coniferous trees.

The contradictory evolution of the beech stands in the area of Crana (first decreasing between 1910 and 1933 and then dramatically increasing from 1933 to 2012) and of the larch stands (increasingly dramatically from 1910 to 1933 and then staying almost constant) probably reflects the difficulties in interpreting the spatial meaning of the symbols in Bär's map. Beside the fact that Johann Bär worked with a very inaccurate topographic map with respect to current maps, a methodological problem arises when trying to compare quantitatively old maps and photographs. Even if our tool makes it now relatively easy, such a comparison remains very delicate since the information contained in these two types of historical sources are only partially compatible. There is in particular a problem in trying to accommodate the criteria for the interpretation of Bär's symbology to the rules used during photo-interpretation and to keep objectivity during map interpretation. Furthermore, for stands located in sectors characterized by a low angle of incidence of the optical ray on the DEM surface, the achieved precision when drawing polygons is inevitably low.

An additional possible source of error is accounted for by the limits of the camera calibration we adopted, where control points were collected through indirect measurements on maps and orthophotos without any in-field verification or survey.

5. Conclusions

The aim of monoplotting is to provide low cost solutions for the execution of fairly accurate measurements and mappings starting from common oblique photographs. As a general trend, monoplotting implies a certain reduction in accuracy, rewarded by gains in terms of flexibility, adaptability and ease of execution of the technique. In fact, it is sufficient to have a single photo and a DEM representing the depicted portion of the landscape, to start the photogrammetric process. With such basic requirements, the monoplotting technique can be successfully applied in many different fields, both for studies in the present (e.g. low-cost process monitoring) as well as for studies on landscape changes in the past (e.g. cartography from historical pictures).

The present study highlighted the suitability of the WSL monoplotting tool to meet such requirements and in particular to make different sources of explicit spatial information on the same cultural heritage object compatible and easily comparable. By editing and georeferencing the categories on Bär's vegetation map and on the old and new photos and by projecting the defined polygons into the orthogonal and photographic perspectives, we were able to effectively compare the state of vegetation in 1910, 1933 and 2012.

The monoplotting tool allowed us, in particular, to bypass differences in terms of perspective and shooting points, thus making it possible to compare the information resulting from the old map and from photographs taken at different times and in different places. All the data plotted on the selected images were georeferenced successfully and imported into the GIS environment where it was easy to carry out the required spatial analysis. In this sense, we can say that the new software makes many different photo-geographical approaches and comparisons possible that are very innovative and promising.

The tool, however, is still a prototype and further suitable improvements are foreseen for the future. In particular, these include:

- the insertion of specific *ArcMap* features (e.g. the possibility to calculate the viewshed, the orthogonal area and the surface area) directly into the monoplotting tool inside our software, so as to avoid the continuous transitions from one working environment to the other;
- the development of advanced features for orthorectifying raster data to georeference oblique terrestrial photographs as originally proposed by Aschenwald et al. (2001) and Corripio (2004);
- the possibility of considering the effect of the terrestrial curvature 0.8 m/km;
- the implementation of a feature for the direct and interactive calculation of the achieved error on each pixel of the treated image.

6. Acknowledgements

We thank the *Federal Archive of historical monuments* (FAHM) at the *National Library* in Bern for providing us with the following photos: 5012 (Crana), 5182 (Gresso), and 5206 (Vergeletto) of the Fundus Rudolf Zinggeler. This research was partially funded by the Locarnese National Park Project and by the *Bristol foundation*. We are grateful to Curtis Gautschi for helpful suggestions.

7. References

Aschenwald, J.; Leichter, K.; Tasser, E.; Tappeiner, U.; 2001. Spatio-temporal landscape analysis in mountainous terrain by means of small format photography: a methodological approach. *IEEE Transactions on Geoscience and Remote Sensing*, 39(4), pp. 885-893.

Bär, J., 1918. Die Vegetation des Val Onsernone (Kanton Tessin). Rascher & Co., Zürich.

Canale, A.; 1958. *Geomorphologie der Valle Onsernone*. Grafica Bellinzona SA; Bellinzona.

Ceruzzi, P.E., 2003. *A history of modern computing*. MIT Press, Cambridge.

Corripio, J.G.; 2004. Snow surface albedo estimation using terrestrial photography. *International journal of remote sensing*, 25(24), pp. 5705-5729.

Doytsher, Y.; Hall, J.K.; 1995. FORTRAN programs for coordinate resection using an oblique photograph and high-resolution DTM. *Computers & Geosciences*, 21(7), pp. 895-905.

Fluehler, M.; Niederoest, J.; Akca, D.; 2005. *Development of an educational software system for the digital monoplotting*, Proceedings of the ISPRS, Working group VI/1 - VI/2 (Tools and Techniques for E-Learning), Potsdam (Germany), June 1-3 2005, 6 pp.

Ghosh, S.K.; 2005. *Fundamentals of computational photogrammetry*. Concept Publishing Company, New Delhi.

Hendrick, L.E.; Copenheaver, C.A.; 2009. Using repeat landscape photography to assess vegetation changes in rural communities of the Southern Appalachian Mountains in Virginia, USA. *Mountain Research and Development*, 29(1), pp. 21-29.

Hodgson, M.E.; Bresnahan, P.; 2004. Accuracy of airborne lidar-derived elevation: empirical assessment and error budget, *International Archives for Photogrammetry and Remote Sensing*, 70(3), pp. 331-339.

Kraus, K.; 1993. Photogrammetry. Vol. 1: Fundamentals and standard processes. Dümmlers, Bonn.

Krebs, P.; Conedera, M.; 2004. La fotografia terrestre: un mezzo di grande efficacia per comprendere il passato e prepararsi al futuro. *Quaderni Grigionitaliani*, 73(4), pp. 342-354.

Kull, C.A.; 2005. Historical landscape repeat photography as a tool for land use change research. *Norwegian Journal of Geography*, 59, pp. 253-268.

Makarovič, B.; 1973. Digital monoplotters. *The ITC journal*, 1973(4), pp. 583-600.

Makarovič, B.; 1982. Data base updating by digital monoplotting, *The ITC journal*, 1982(4), pp. 384-390.

Mikhail, E.M. ; Bethel, J.S.; McGlone, J.C.; 2001. *Introduction to modern photogrammetry*. John Wiley & Sons, New York.

Miller, C.L.; Laflamme, R.A. ; 1958. The digital terrain model - theory and application. *Photogrammetric Engineering and Remote Sensing*, 24, pp. 433-442.

Mitishita, E.A.; Machado, A.L.; Habib, A.F.; Gonçalves, G.; 2004. 3D monocular restitution applied to small format digital airphoto and laser scanner data. Proceedings of Commission III, XXth ISPRS Congress (International Society for Photogrammetry and Remove Sensing), Istanbul (Turkey), July 12-23, 2004. *Remote Sensing and Spatial Information Sciences*, 35(B3), pp. 70-75.

Muster, S.; Elsenbeer, H.; Conedera, M.; 2007. Small-scale effects of historical land use and topography on post-cultural tree species composition in an Alpine valley in southern Switzerland. *Landscape Ecology*, 22(8), pp. 1187-99.

Nyssen, J.; Haile, M.; Naudts, J.; Munro, N.; Poesen, J.; Moeyersons, J.; Frankl, A.; Deckers, J.; Pankhurst, R.; 2009. Desertification? Northern Ethiopia re-photographed after 140 years. *Science of The Total Environment*, 407(8), pp. 2749-2755.

Samtaney, R.; 1999. A method to solve interior and exterior camera calibration parameters for image resection. NASA Technical Reports.

Strausz, D.A.; 2001. An application of photogrammetric techniques to the measurement of historic photographs. Oregon State University, Department of Geosciences.

Waldhäusl, P.; Hochstöger, F.; 1990. Monoplotting: Einzelbildauswertung für die Beobachtung von Veränderungen auf der Geländeoberfläche. In: *VI. Internationale Geodätische Woche Obergurgl*, Institut für Geodäsie, Innsbruck, pp. 137-154.

Wolf, P.R.; Dewitt, B.A.; 2000. *Elements of photogrammetry with applications in GIS*. McGraw Hill, New York.